Communications in Physics, Vol. 28, No. 1 (2018), pp. 51-60
DOI:10.15625/0868-3166/28/1/11080

TRAPPING ELECTRONS IN A CIRCULAR GRAPHENE QUANTUM DOT WITH GAUSSIAN POTENTIAL

NHUNG T. T. NGUYEN†

Institute of Physics, Vietnam Academy of Science and Technology,
10 Dao Tan, Ba Dinh, Hanoi, Vietnam

†*E-mail:* ntnhung@iop.vast.ac.vn

Received 16 January 2018
Accepted for publication 12 March 2018
Published 26 March 2018

Abstract. *We study how the trapping time of an electron in a circular graphene quantum dot depends on the electron's angular momentum and on the parameters of the external Gaussian potential used to induce the dot. The trapping times are calculated through a numerical determination of the quasi-bound states of electron from the two-dimensional Dirac-Weyl equation. It is shown that on increasing the angular momentum, not only the trapping time decreases but also the trend of how the trapping time depends on the effective radius of the dot changes. In particular, as the dot radius increases, the trapping time increases for $m < 3$ but decreases for $m > 3$. The trapping time however always decreases upon increasing the potential height. It is also found that the wave functions corresponding to the states of larger trapping times or higher m are more localized in space.*

Keywords: quasi-bound state, localization, trapping time.

Classification numbers: 73.63.Kv, 73.23.−b, 81.05.Uw .

I. INTRODUCTION

Graphene is a two-dimensional conducting material made up from a single layer of carbon atoms with unique electronic properties [1]. Due to the special sublattice symmetry of graphene, electrons in graphene under low energy excitations can be considered as quasi-relativistic massless chiral fermions, which are formally described by the Dirac-Weyl equation. Anomalous Hall effect [2], absence of backscattering and Klein paradox [3] are examples of the most intriguing properties possessed by the quasi-relativistic electrons in graphene. In the Klein paradox, an electron approaching a potential barrier with a zero transverse momentum will tunnel through the barrier with a transmission probability equal to unity independent of the barrier height. Due to the Klein tunneling, it is impossible to localize electrons in a small region of graphene as in a conventional quantum dot. Fortunately, electrons can still be trapped in such a region for some finite time that is hopefully long enough to execute an electronic operation by applications [4].

Experimentally, there are several methods of creating graphene quantum dots. The electron beam lithography is one of them, in which a preferred structure is cut from a graphene flake [5]. However, producing a graphene quantum dot with nano-size precise termination is an arduous task. It is well known that the electronic properties of graphene nanostructures strongly depend on the geometry of the graphene edges, such as zigzag or armchair [6]. For applications, it is desirable to have the dots whose electronic properties are not sensitive to the edges of the structures. Therefore, other methods of fabricating quantum dots by electrically confining charge carriers in a small region of a graphene sheet have been developed. Zhao *et al.* [7] created nano-sized electron cavities in graphene, which are circular p-n junctions by implementing the scanned electron tunneling (STM) probe. This method uses a planar back gate, which tunes the carrier density of the whole graphene sheet, and the STM tip, considered as a top gate, that tunes the carrier density just below the tip. As the consequence of this tuning, confined electronic states are obtained. In the study of Lee et al. [8], the graphene quantum dots were fabricated using a technique involving local manipulation of defect charge within the insulating substrate beneath a graphene monolayer. In the experiment by Gutierrez et al. [9], nearly circular graphene quantum dots were induced by an engineered copper substrate that leads to different potential energies inside and outside the dot. Since the graphene sheet that contains an electrically induced graphene quantum dot has a much larger size than the dot, the electronic properties of the dot are considerably not affected by the edges of the graphene sheet.

The finite trapping time of electron in an electrically induced graphene quantum dot is often obtained through the description of the electron's quasi-bound states of complex energies [4]. For a quasi-bound state of energy E, the characteristic trapping time is given by $\tau = \hbar/|\operatorname{Im} E|$, where $\operatorname{Im} E$ is the imaginary part of E. The real and imaginary parts of E also correspond to the position and the width, respectively, of a resonance peak in the electron density of states [10]. There have been theoretical studies of graphene quantum dots of various potential shapes. Hewageegana and Apalkov [11] shows that in a circular graphene quantum dot with a sharp rectangular potential, among the quasi-bound states, strongly localized states can exist due to interference effect. In particular, electrons having an energy equal to the height of the confinement potential are fully localized, i.e. with infinite trapping time, if the potential height corresponds to a root of a Bessel function. The study of Chen et al. [12] suggests that the trapping time of electron in graphene

quantum dots increases with the smoothness of the confinement potential given by a power function and the electron's angular momentum. The quantum dots induced by trapezoidal potential have been studied in Ref. [13] showing that the trapping time increases when the slope of changing part of the potential decreases. Note that differently fabricated quantum dots may correspond to different potential shapes. It has been shown [8] that the experimental charge density map for a graphene quantum dot has a smoothly changing profile at the p-n junction boundary, suggesting that it is induced by a smooth potential. Other fabricated graphene quantum dots are claimed to have sharp boundaries of the boundary size $\sim$1 nm [9]. Thus, the shape of the confinement potential can be monitored by the method of fabrication, even though experimentally it is not possible to determine the exact form of a potential.

In the present work, we adopt a Gaussian potential to study the trapping of electrons in electrically induced graphene quantum dots. It has been suggested that the Gaussian shape potential better reflects the potential profile in graphene bipolar junctions than other types of potential due to its smoothness [14, 15]. This gives us a motivation to apply this potential to the quantum dots. We will find the solutions of the Dirac-Weyl equation numerically by using the Runge-Kutta method and by scanning a complex energy plane. The effects of dot radius and potential heights as well as that of angular momentum on the trapping time, the wave function and the density of states of electron will be investigated.

II. METHODS

Model of graphene quantum dot

We consider a model of graphene quantum dot induced by a Gaussian shape confinement potential

$$U(r) = U_0 \exp(-r^2/d^2) \,, \tag{1}$$

where U_0 is the potential height, r is the radial distance from the center of the dot and d is the effective dot radius. The Hamiltonian of a single electron in graphene with such a potential has a Dirac-Weyl form and is given by

$$\hat{H} = v_F \vec{\sigma} \cdot \hat{p} + U(r) \,, \tag{2}$$

where $v_F \approx 10^6$ m s^{-1} is the Fermi velocity, $\vec{\sigma} = (\sigma_x, \sigma_y)$ are spin Pauli matrices and $\hat{p} = -i(\partial_x, \partial_y)$ is a 2D momentum operator. In polar coordinates with r and ϕ as the radial distance and azimuthal angle, respectively, the Hamiltonian can be written as

$$\hat{H} = \begin{pmatrix} U(r) & -i\hbar v_F e^{-i\phi}\left(\partial_r - \frac{i}{r}\partial_\phi\right) \\ -i\hbar v_F e^{i\phi}\left(\partial_r + \frac{i}{r}\partial_\phi\right) & U(r) \end{pmatrix} . \tag{3}$$

The wave function ψ of electron satisfies the Dirac-Weyl equation

$$\hat{H}\psi = E\psi \,, \tag{4}$$

with E the electron's energy. Due to the cylindrical symmetry of the potential, we consider the solutions of (4) in the following form:

$$\psi(r,\phi) = \begin{pmatrix} e^{i(m-1)\phi}\chi_A(r) \\ e^{im\phi}\chi_B(r) \end{pmatrix} , \tag{5}$$

where the angular momentum number m has integer values; $\chi_A(r)$ and $\chi_B(r)$ are the radial parts of the spinor components of the wave function corresponding to the projections of the latter on the

graphene sublattices A and B, respectively. The energy E is assumed to have complex values, to allow for the non-stationary (quasi-bound) solutions.

Putting (5) into (4) we get two coupled differential equations:

$$\frac{\partial \chi_B(r)}{\partial r} + \left(\frac{m}{r}\right)\chi_B(r) = i\left(\frac{E-U(r)}{\hbar v_F}\right)\chi_A(r)\,, \tag{6}$$

$$\frac{\partial \chi_A(r)}{\partial r} - \left(\frac{m-1}{r}\right)\chi_A(r) = i\left(\frac{E-U(r)}{\hbar v_F}\right)\chi_B(r)\,. \tag{7}$$

For r large enough ($r \gg d$) to consider that $U(r) = 0$, it can be shown that the solutions of (6) and (7) representing outgoing waves are

$$\chi_A^\star(r) = \alpha H_{m-1}^{(1)}\left(\frac{Er}{\hbar v_F}\right)\,, \tag{8}$$

$$\chi_B^\star(r) = i\alpha H_m^{(1)}\left(\frac{Er}{\hbar v_F}\right)\,, \tag{9}$$

where $H_m^{(1)}(x)$ is the Hankel function of the first kind of the order m and α is a normalizing constant.

In calculations, energy will be given in meV whereas length will be given in units of a with $a = 0.246$ nm being the graphene lattice constant.

Runge-Kutta method

In order to obtain the solutions for a full range of r, we use the 4th order Runge-Kutta method [16] to numerically integrate the coupled equations (6) and (7). To illustrate the method, consider a system of 2 ordinary coupled differential equations:

$$x_1' = f_1(t, x_1, x_2)\,, \tag{10}$$

$$x_2' = f_2(t, x_1, x_2)\,, \tag{11}$$

where $x_1 = x_1(t)$, $x_2 = x_2(t)$ and the left hand sides are their first derivatives with respect to t. Let

$$\mathbf{X} = \begin{bmatrix} x_1 \\ x_2 \end{bmatrix} \qquad \text{and} \qquad \mathbf{F}(t, \mathbf{X}) = \begin{bmatrix} f_1 \\ f_2 \end{bmatrix}\,. \tag{12}$$

The 4th order Runge-Kutta method is given by [16]

$$\mathbf{X}(t+h) = \mathbf{X}(t) + \frac{1}{6}(\mathbf{K}_1 + 2\mathbf{K}_2 + 2\mathbf{K}_3 + \mathbf{K}_4)\,, \tag{13}$$

where h is an integration step and

$$\mathbf{K}_1 = h\mathbf{F}(t, \mathbf{X})\,, \tag{14}$$

$$\mathbf{K}_2 = h\mathbf{F}\left(t + \frac{h}{2}, \mathbf{X} + \frac{\mathbf{K}_1}{2}\right)\,, \tag{15}$$

$$\mathbf{K}_3 = h\mathbf{F}\left(t + \frac{h}{2}, \mathbf{X} + \frac{\mathbf{K}_2}{2}\right)\,, \tag{16}$$

$$\mathbf{K}_4 = h\mathbf{F}(t + h, \mathbf{X} + \mathbf{K}_3). \tag{17}$$

For our quantum dot problem, we have considered the wave functions in the range of $r \in [r_{\min}, r_{\max}]$, where $r_{\min}$ is a small value near zero and $r_{\max}$ is a large value much larger than the dot radius. For a given value of E, the wave function at $r = r_{\max}$ is calculated from equations (8) and (9). The solution for the full range of r is obtained by performing a backward Runge-Kutta integration, i.e. shooting from $r_{\max}$ to $r_{\min}$ with a negative integration step

$$h = \frac{r_{\min} - r_{\max}}{N} < 0 \,, \tag{18}$$

where N is the number of integration steps. We look for solutions which do not diverge near $r = 0$. This is done by considering the following score function

$$q(E) = \log\left(|\chi_A(r_{\min})|^2 + |\chi_B(r_{\min})|^2\right) \tag{19}$$

in the complex energy plane of $\mathrm{Re}\,E$ and $\mathrm{Im}\,E$. The solutions corresponding to the quasi-bound states are such that q is a local minimum in this plane. In our calculations, we choose $r_{\max} = 10\,d$, $r_{\min}$ varying from $0.01d$ to $0.05d$, and the number of integration steps N is chosen such that $h \approx -a$. Typically, as m increases we need also to increase $r_{\min}$ in order to avoid divergence at the small r due to numerical errors.

III. RESULTS AND DISCUSSION

Fig. 1 shows the complex energy spectrum of the quasi-bound states of electron in graphene quantum dot for various angular momentum numbers m of electron and effective radii d of the dot. The potential height in these cases is fixed to be $U_0 = 200$ meV. For each values of m and d, there is a certain number of energy values found in the complex energy plane shown as $(\mathrm{Re}\,E)$ versus $(-\mathrm{Im}\,E)$. Note that here $\mathrm{Im}\,E < 0$ is due to the fact that we have a potential barrier ($U_0 > 0$) instead of a potential well. This means that the localized particles are holes instead of electrons, but since in graphene these two types of particles are fully equivalent at low energy excitations we will refer the localized particles as electrons only. The spectra show that for given m and d, the smallest values of $(-\mathrm{Im}\,E)$ are observed for the states of the lowest and the highest $(\mathrm{Re}\,E)$. One can see that as m increases the range of $(-\mathrm{Im}\,E)$, in which the energy values are found, decreases rapidly. In particular, for m increases from 2 to 8, the $(-\mathrm{Im}\,E)$ range decreases almost 300 times. This result is in agreement with the result reported in Ref. [12] for a quantum dot with different confinement potential, and confirms that the trapping time increases quickly with m.

Here, we find that the trend of how the trapping time depends on the dot radius also depends on m. For $m = 2$, it is shown that $(-\mathrm{Im}\,E)$ decreases as the dot radius d increases from $200\,a$ to $400\,a$ (Fig. 1A), indicating an increase of trapping time on increasing the dot radius. On the other hand, for $m > 3$ an inverse trend is observed, i.e. $(-\mathrm{Im}\,E)$ decreases when d decreases (Figs. 1C and 1D). The number of states however also decreases quickly with d. The case of $m = 3$ corresponds to the crossover of the trend as for this case the values of $(-\mathrm{Im}\,E)$ for different dot radii are quite close. Thus, electrons are better confined when m increases but also for $m > 3$ the trapping time decreases with the dot radius. Note that technically it is more difficult to fabricate dots of small size.

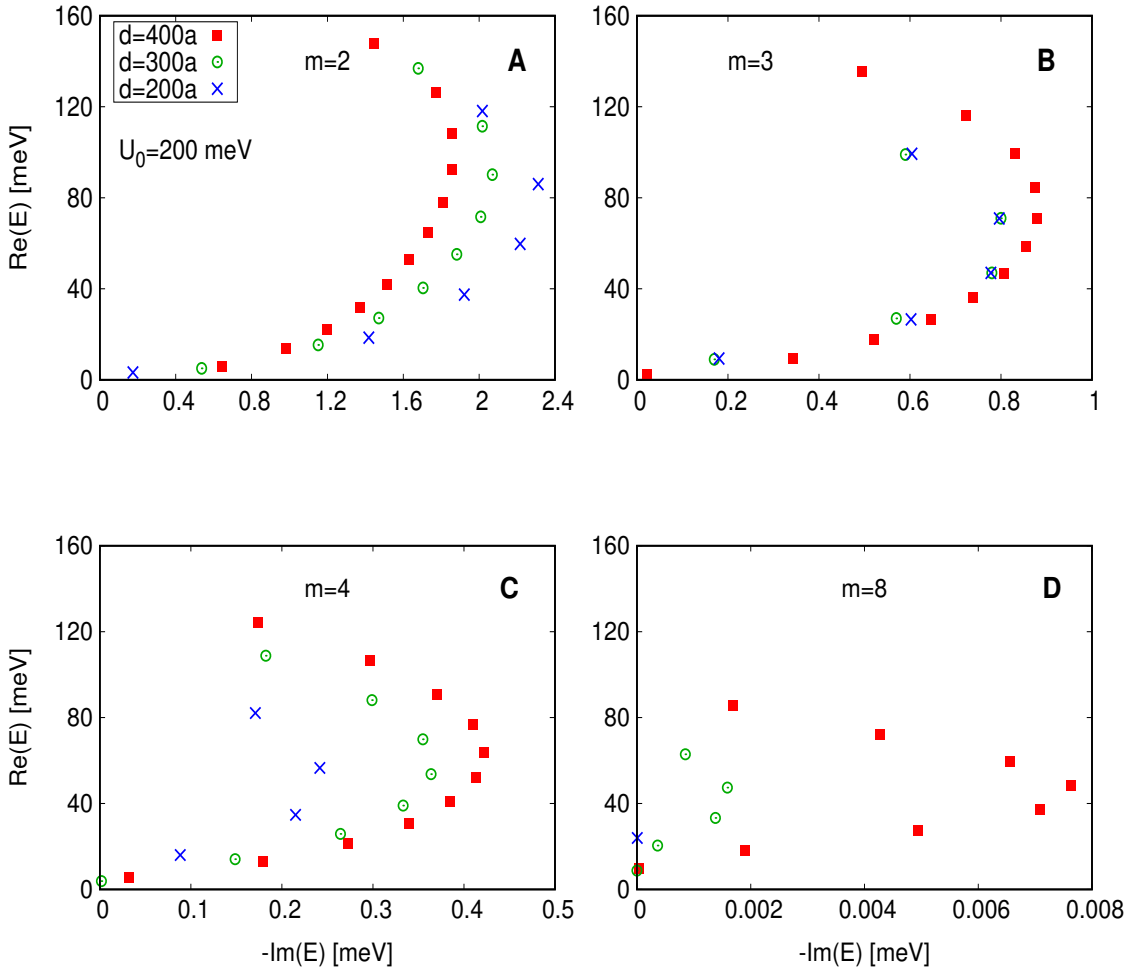

Fig. 1. Real vs. imaginary part of the energies of the quasi-bound states for $U_0 = 200$ meV and varying dot radius d and azimuthal quantum number m. The panels show the data for $d = 200\,a$ (crosses), $300\,a$ (circles) and $400\,a$ (squares) for $m = 2$ (A), $m = 3$ (B), $m = 4$ (C) and $m = 8$ (D) as indicated.

We now fix the dot radius to be $d = 400\,a$ and study the dependence of trapping time on the potential height U_0. Fig. 2 shows that on changing U_0 from 200 meV to 150 meV and then to 100 meV, $(-\mathrm{Im}\,E)$ decreases (the trapping time increases) but also the number of energy values decreases. This tendency is consistent for all values of m considered. Thus, on lowering the potential barrier one can localize better but with less electrons.

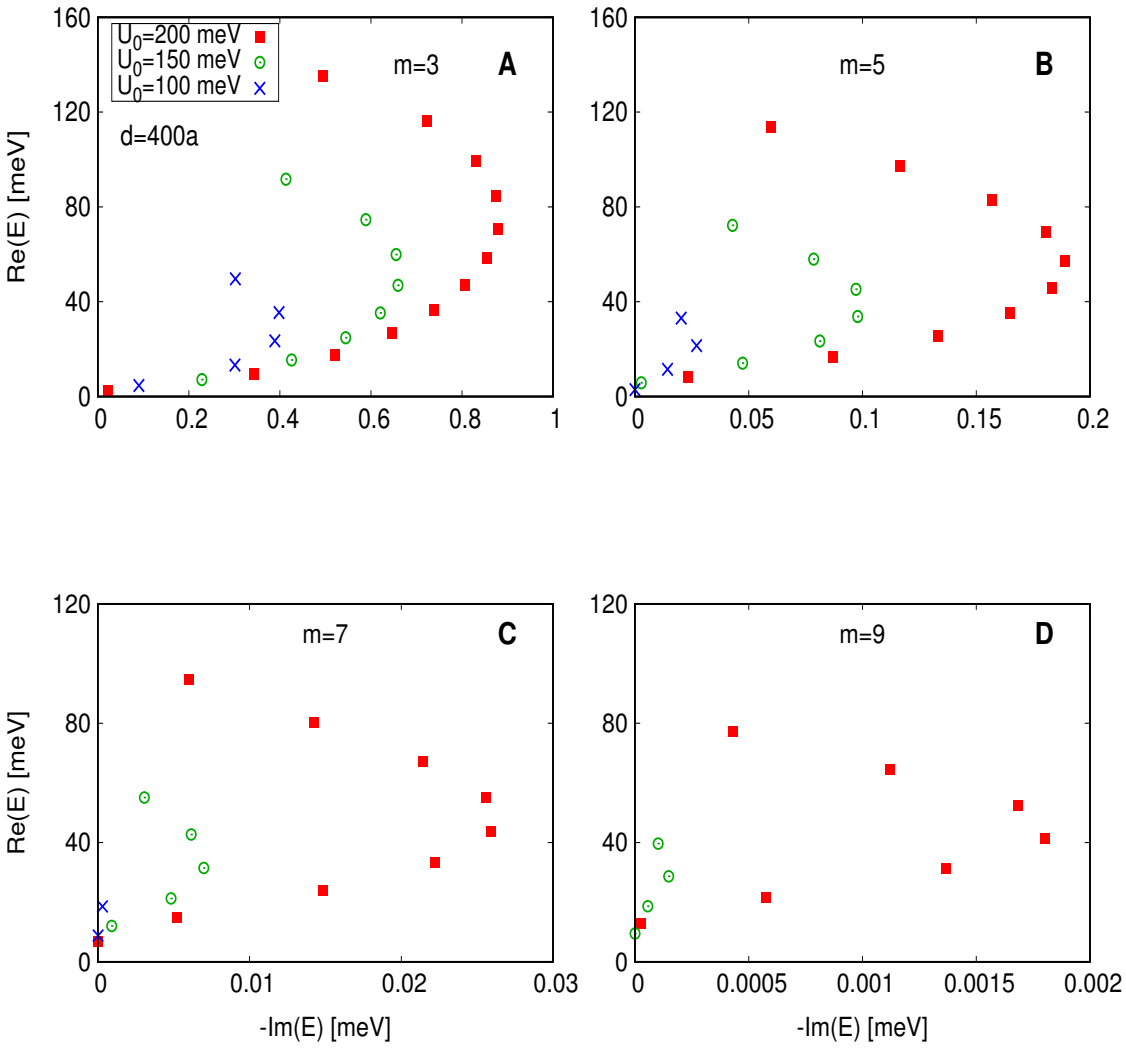

Fig. 2. Real vs imaginary part of the energies of the quasi-bound states for quantum dot of $d = 400a$ and varying U_0 and m. The panels show the data for $U_0 = 200$ meV (squares), 150 meV (circles) and 100 meV (crosses) for $m = 3$ (A), $m = 5$ (B), $m = 7$ (C) and $m = 9$ (D) as indicated.

Fig. 3 shows the radial parts of the two-component spinor wave functions obtained for several quasi-bound states of different m. It is shown that as m increases the amplitude of the wave function inside the dot increases while the amplitude outside the dot decreases, which means that electron is better localized in space at higher angular momentum. Note that the higher m states are also associated with longer trapping times. Thus, there is some correlation between the trapping time and the localization in space of the trapped electrons.

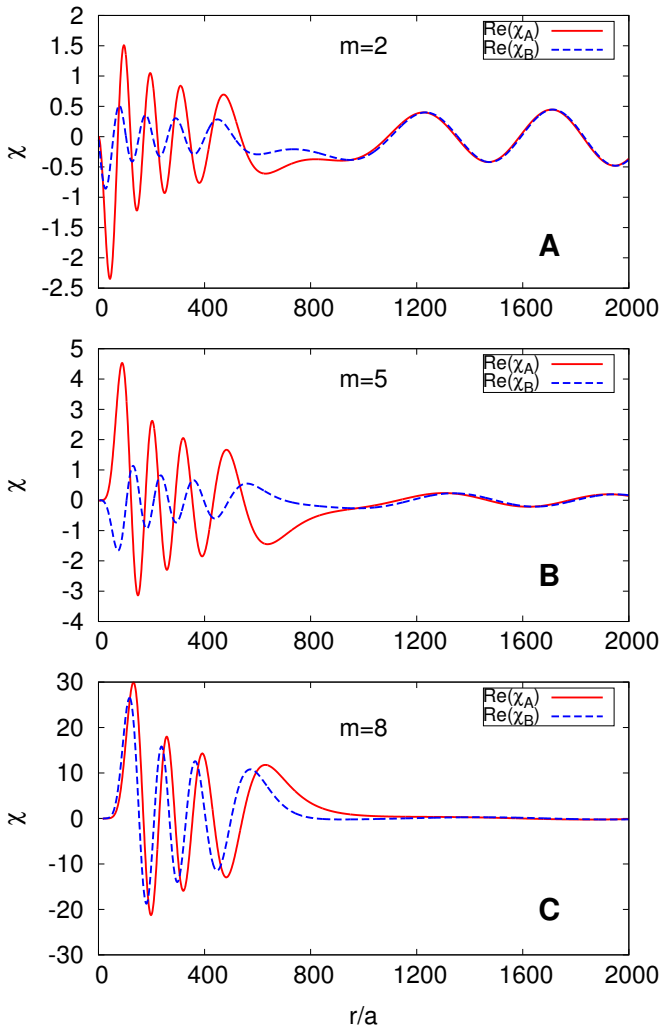

Fig. 3. Examples of the radial wave function for $m = 2$ (A), $m = 5$ (B) and $m = 8$ (C) with $d = 400\,a$ and $U_0 = 200$ meV. For the case in A: $\mathrm{Im}\,E = -1.3706$ meV, $\mathrm{Re}\,E = 31.6851$ meV. For the case in B: $\mathrm{Im}\,E = -0.1331$ meV, $\mathrm{Re}\,E = 25.4893$ meV. For the case in C: $\mathrm{Im}\,E = -0.00189$ meV, $\mathrm{Re}\,E = 18.2140$ meV.

In Fig. 4, we show the density of states for the quantum dots of $d = 400\,a$ with $U_0 = 200$ meV and $U_0 = 300$ meV and for $m = 2$ and $m = 6$. The density of state for a given quantum dot and for a given m is calculated as [11]

$$g(E) = \frac{1}{\pi} \sum_{n=1}^{K} \frac{-\mathrm{Im}\,E_n}{|E - E_n|^2}\,, \tag{20}$$

where E is a real energy variable, E_n is the complex energy of a quasi-bound state with an index n and K is the total number of the quasi-bound states obtained in the calculation. It is shown that the resonance peaks are quite broad for $m = 2$ and much narrower for $m = 6$. This finding is consistent with the decrease of $(-\mathrm{Im}\,E)$ values on increasing m. Fig. 4 also shows that there are more resonance peaks for the dots of larger U_0. In fact, the position and the width of the resonance peaks should correspond to the values of $(\mathrm{Re}\,E)$ and $(-\mathrm{Im}\,E)$.

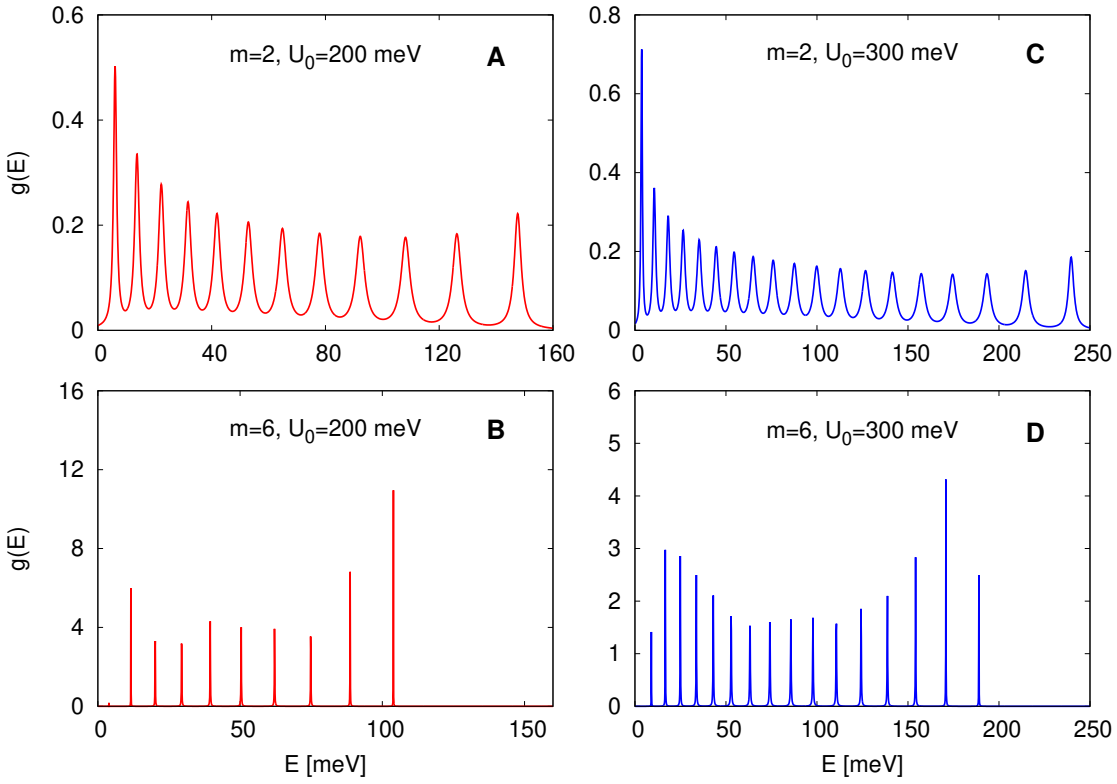

Fig. 4. Density of states for quantum dots with $d = 400a$. The panels shown are for $U_0 = 200$ meV and $m = 2$ (A), $U_0 = 300$ meV and $m = 2$ (B), $U_0 = 200$ meV and $m = 6$ (C), and $U_0 = 300$ meV and $m = 6$ (D).

IV. CONCLUSION

In this paper, we have studied the trapping times of electron in graphene quantum dots induced by a Gaussian potential. We have shown that the trapping time increases with the angular momentum number m of electron. We have also shown that there are opposite trends of how the trapping time changes with the dot radius for low and high m values, while the trapping time always decreases on increasing the potential height for all m. The calculated wave functions of the

quasi-bound states show that an electron poorer localized in time, i.e. having longer trapping time, is better localized in space. Our results also indicate that there is a tradeoff between the capabilities of a graphene quantum dot to trap more electrons in the dot and to trap them more efficiently in time. In other words, larger and induced by stronger potential quantum dots can accommodate more electrons but also trap them in shorter times.

ACKNOWLEDGMENTS

The author is indebted to Prof. V. Lien Nguyen, H. Chau Nguyen, and Huy-Viet Nguyen for fruitful discussions. This research is funded by Vietnam National Foundation for Science and Technology Development (NAFOSTED) under grant number 103.02-2015.48.

REFERENCES

[1] A. C. Neto, F. Guinea, N. M. Peres, K. S. Novoselov and A. K. Geim, *Rev. Mod. Phys.* **81** (2009) 109.
[2] F. Guinea, M. Katsnelson and A. Geim, *Nat. Phys.* **6** (2010) 30.
[3] M. Katsnelson, K. Novoselov and A. Geim, *Nat. Phys.* **2** (2006) 620.
[4] A. Matulis and F. Peeters, *Phys. Rev. B* **77** (2008) 115423.
[5] A. El Fatimy, R. L. Myers-Ward, A. K. Boyd, K. M. Daniels, D. K. Gaskill and P. Barbara, *Nat. Nanotech.* **11** (2016) 335.
[6] V. H. Nguyen, V. Nam Do, A. Bournel, V. L. Nguyen and P. Dollfus, *J. Appl. Phys.* **106** (2009) 053710.
[7] Y. Zhao, J. Wyrick, F. D. Natterer, J. F. Rodriguez-Nieva, C. Lewandowski, K. Watanabe, T. Taniguchi, L. S. Levitov, N. B. Zhitenev and J. A. Stroscio, *Science* **348** (2015) 672–675.
[8] J. Lee, D. Wong, J. Velasco Jr, J. F. Rodriguez-Nieva, S. Kahn, H.-Z. Tsai, T. Taniguchi, K. Watanabe, A. Zettl, F. Wang et al., *Nat. Phys.* **12** (2016) 1032.
[9] C. Gutiérrez, L. Brown, C.-J. Kim, J. Park and A. N. Pasupathy, *Nat. Phys.* **12** (2016) 1069.
[10] H. C. Nguyen, N. T. Nguyen and V. L. Nguyen, *J. Phys.: Cond. Matt.* **29** (2017) 405301.
[11] P. Hewageegana and V. Apalkov, *Phys. Rev. B* **77** (2008) 245426.
[12] H.-Y. Chen, V. Apalkov and T. Chakraborty, *Phys. Rev. Lett.* **98** (2007) 186803.
[13] H. C. Nguyen, N. T. Nguyen and V. L. Nguyen, *J. Phys.: Cond. Matt.* **28** (2016) 275301.
[14] S. D. Sarma, S. Adam, E. Hwang and E. Rossi, *Rev. Mod. Phys.* **83** (2011) 407.
[15] N. T. Nguyen, D. Q. To and V. L. Nguyen, *J. Phys.: Cond. Matt.* **26** (2013) 015301.
[16] E. Cheney and D. Kincaid, *Numerical mathematics and computing*, 5 ed., Brooks Cole, 2004.